J Therm Anal Calorim (2017) 128:1305–1312
DOI 10.1007/s10973-016-6045-y

Synthesis, characterization of nanosized $CoAl_2O_4$ and its electrocatalytic activity for enhanced sensing application

Raluca Dumitru[1] · **Florica Manea**[1] · **Lavinia Lupa**[1] · **Cornelia Păcurariu**[1] ·
Adelina Ianculescu[2] · **Anamaria Baciu**[1] · **Sorina Negrea**[1]

Received: 12 September 2016 / Accepted: 8 December 2016

Abstract Nanosized cobalt aluminate ($CoAl_2O_4$) was prepared by thermolysis of heteronuclear coordination compound, namely $[Al_2Co(C_2O_4)_4(OH_2)_6]$. The synthesized precursor was characterized by chemical analysis, vibrational spectra and thermal analysis. The cobalt aluminate obtained after a heating treatment of the precursor at 700 °C was characterized by IR, XRD, TEM coupled with SAED measurements. Two types of carbon-based electrodes, glassy carbon and boron-doped diamond electrodes were decorated with the obtained cobalt aluminate in order to enhance the electroanalytical performance for the tetracycline (TC) detection in the aqueous solutions. Cyclic voltammetry technique was used to determine the effect of the nanosized $CoAl_2O_4$ on the electrochemical oxidation of TC and as consequence, for TC detection at both carbon-based electrodes. The obtained cobalt aluminate exhibited the electrocatalytic activity toward TC detection in direct relation with the type of the carbon substrate, which allowed enhancing the electroanalytical parameters of TC detection in the aqueous solution.

Keywords Cobalt aluminate · Tetracycline · Oxalate · Electrochemical detection · Electrocatalytic activity

Introduction

The spinel-type oxides, due to their chemical, thermal stability and high mechanical resistance, represent a new class of materials with a wide range of applications, such as: magnetic devices, ceramics, thin films, catalysis and adsorbent materials [1–6]. Among this class of materials, cobalt aluminate ($CoAl_2O_4$) received a lot of attention due to its scientific properties being used as: electrochemical sensor [7]; ceramic pigment [8, 9]; thin films [10]; and catalyst [11]. From these reasons, a lot of researchers focused to find the best method of the spinel obtaining, which could be processed at lower temperatures and to control homogeneity, purity, size and shape of the product. Deraz et al. [7] tried to obtain $CoAl_2O_4$ nano-composite via glycine-assisted combustion method. They controlled the size of $CoAl_2O_4$ nano-crystals by tuning the molar ratio of CoO to Al_2O_3. In general, besides $CoAl_2O_4$, the obtained product contains also, CoO particles. Ummartyotin et al. [12] used the metal complex method in order to prepare $CoAl_2O_4$ spinel. The metal complex method was used also in order to prepare $CoAl_2O_4$ spinel [12]. Using this method the spinel was obtained through the calcination of the Co–Al–TEA in propan-1-ol complex at high temperatures of 800–1200 °C. Another method reported in the literature for the spinel obtaining is based on a chemical route in the Pechini method which also involved calcination at 1000 °C [13]. $CoAl_2O_4$ spinel as a single-phase was obtained through thermal decomposition at 1000 °C of polynuclear multimetallic compounds containing tartarate and gluconate anions as ligands, respectively [14]. Nanosized

---

Electronic supplementary material The online version of this article (doi:10.1007/s10973-016-6045-y) contains supplementary material, which is available to authorized users.

✉ Raluca Dumitru
raluca.voda@upt.ro

[1] Faculty for Industrial Chemistry and Environmental Engineering, University “Politehnica” of Timisoara, Piata Victoriei No. 2, 300006 Timisoara, Romania

[2] Department of Oxide Materials Science and Engineering, Faculty of Applied Chemistry and Materials Science, Polytehnic University of Bucharest, Gh. Polizu Street No. 1-7, 011061 Bucharest, Romania

cobalt aluminate spinel powders were prepared by the sol–gel and sol–gel-hydrothermal methods using aluminum secbutoxide, cobalt salts and nitric acid as oxides precursors to form sols and gels [15]. The temperature for obtaining the blue $CoAl_2O_4$ was about 1000 and 250 °C by using the sol–gel and respective, sol–gel-hydrothermal methods.

Various cobalt-based nanostructures have been proved as promising materials for the electrochemical detection of various compounds [16–18]. In general, in comparison with the macroelectrodes, nanoparticles-modified electrodes exhibit several advantages, e.g., catalytic activity, high effective surface area and enhancement of mass control [19, 20]. The carbon-based electrodes are widely used in electroanalysis due to their good mechanical resistance, high reproducibility and stability, good electrical conductivity [18], and they are suitable for modification with nanoparticles as chemically modified electrodes (CMEs). Glassy carbon and boron-doped diamond electrodes have been reported for many applications in electroanalysis without any modifications [21] and also modified with nanoparticles [17, 22].

The aim of this study was obtaining and testing nanosized cobalt aluminate in sensing applications. The precursor of the cobalt aluminate was obtained by a new unconventional method, through the reaction of 1,2-ethanediol with $Al(NO_3)_3{\cdot}9H_2O$ and $Co(NO_3)_2{\cdot}6H_2O$ in the presence of nitric acid. The electrocatalytic activity of cobalt aluminate nanoparticles was tested toward tetracycline oxidation envisaging their sensing applications. Tetracycline, as model of the antibiotics class, was chosen as target analyte for the detection testing using nanosized cobalt aluminate-modified glassy carbon (Co–Al–GC) and boron-doped diamond (Co–Al–BDD) electrodes.

Experimental

Materials and methods

All chemicals of analytical reagent grade from Merck, Germany were used for the synthesis of coordination compound, i.e., $Al(NO_3)_3{\cdot}9H_2O$, $Co(NO_3)_2{\cdot}6H_2O$, 1,2-ethanediol and 2 M HNO_3 solution were used.

The IR spectra (KBr pellets) of the compound and of the decomposition products were recorded on a Jasco FTIR spectrophotometer, in the range of 4000–400 cm^{-1}. The thermal behavior of the sample was studied using a NETZSCH-STA 449C instrument, in the range of 25–1000 °C with a heating rate of 10 K min^{-1}, using alumina crucibles. The experiments were carried out in artificial air, at a flow rate of 20 mL min^{-1}; the mass of the sample was about 16 mg.

The oxides were characterized by X-ray diffraction (XRD) analysis. The powder X-ray diffraction patterns of the decomposition products were recorded at room temperature with a XRD using a Rigaku Ultima IV diffractometer, using Cu K_α radiation ($\lambda = 1.5418$ Å). For the determination of the average crystallite size it has been used Scherrer formula: $D = [0.91\lambda/(\beta\cos\theta)] \times 57.32$, where D is the crystallite size, λ the wavelength (Cu K_α), β the corrected half-width obtained using α quartz as reference and the Waren formula and θ is the diffraction angle of the most intense diffraction peak.

In order to analyze the powders morphology and crystallinity degree, and to check its chemical composition and purity, TEM and HRTEM coupled with SAED (surface area electron diffraction) investigations were performed using a high-resolution transmission electron TECNAI F30 S-Twin microscope.

Synthesis of the coordination compound

An aqueous solution containing ethanediol, aluminum nitrate, cobalt nitrate and nitric acid (2 M) in a molar ratio x:2:1:y where $x \geq 3$ and $y \geq 2$ is heated in a water bath. The reaction is completed when no more gas evolving is observed. The obtained solid reaction product is purified by washing with acetone and maintained in air until constant mass. The reaction yield is nearly quantitative (>90%). The metal content was determined by the atomic absorption spectrophotometry (VARIAN Spectra 110 spectrophotometer). Carbon and hydrogen were analyzed using a Carlo Erba 1108 elemental analyzer. $Al_2CoC_8O_{22}H_{12}$ calcd./found Al%: 9.42/9.55; Co%: 10.28/10.43; C%: 16.76/16.93; H%: 2.09/2.23.

Identification of oxalate anion. The solid oxalic acid ($H_2C_2O_4{\cdot}2H_2O$) obtained after the treatment of the compounds solutions with R-H cationite (Purolite C-100) for metallic cations retention and the evaporation of the remained solution was subjected to the following identification procedures: (1) elemental analysis, (2) FTIR spectroscopy: the spectrum is similar with the one reported by the literature for the oxalic acid [23] (Electronic Supplementary Material) and (3) specific reactions [24].

Testing in sensing application

The electrochemical measurements were carried out using an Autolab potentiostat/galvanostat PGSTAT 302 (Eco Chemie, The Netherlands) controlled with GPES 4.9 software and a three-electrode cell, with a saturated calomel electrode as reference electrode, platinum contraelectrode and the cobalt aluminate-decorated carbon-based working electrode. Commerical glassy carbon (GC) and boron-doped diamond (BDD) electrodes were decorated with the obtained cobalt aluminate by simple immersion within an aqueous suspension (10 mg mL^{-1}) and decorated electrodes were obtained, i.e., cobalt aluminate-decorated GC (Co–Al–GC) and cobalt aluminate-decorated boron-doped diamond (Co–Al–BDD). The electrocatalytic activity of cobalt aluminate was tested for the detection of tetracycline (TC) in aqueous solution using cyclic voltammetry (CV) technique. Sensitivity for TC detection is determined as the slope of a linear dependence between the current corresponding to the TC oxidation peak and the TC concentration based on the calibration plots. Tetracycline (TC) was provided by Antibiotice Iasi, Romania. The stock solution was prepared using ethanol (PAM Corporation, Romania) and 0.1 M NaOH solution (Merck, Germany) in a volume ratio of 1:1 to obtain 0.1 mM TC solution. The supporting electrolyte was 0.1 M Na_2SO_4 solution, prepared using Na_2SO_4 of analytical purity (Merck, Germany) with distilled water.

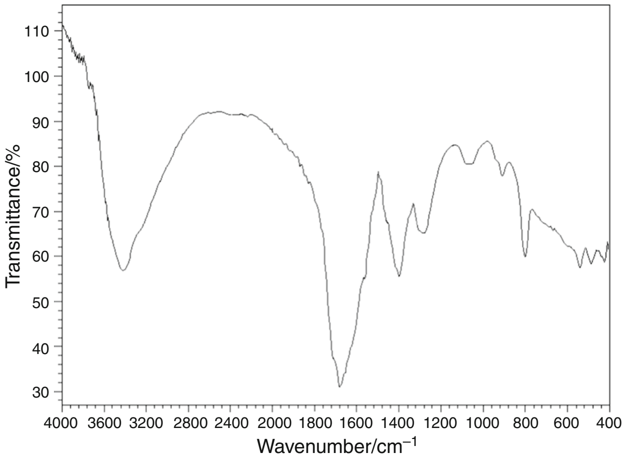

Fig. 1 IR vibrational spectrum of $[Al_2Co(C_2O_4)_4(OH_2)_6]$ compound

Results and discussion

Synthesis and characterization of the coordination compound precursor

The method for the synthesis of coordination compound precursor is based on the redox reaction between 1,2-ethanediol and nitrate ion, in the presence of nitric acid (2 M):

$$12C_2H_4(OH)_2+6\left(\left[Al(OH_2)_6\right]^{3+}+3NO_3^-\right) + 3\left(\left[Co(OH_2)_6\right]^{2+}+2NO_3^-\right) + 8(H^+ + NO_3^-) \rightarrow 3Al_2Co(C_2O_4)_4\cdot 6H_2O_{(s)} + 32NO_{(g)} + 76H_2O_{(g)}$$

The role of 2 M HNO_3 solution was to reduce as much as possible the hydrolysis of $[Al(OH_2)_6]^{3+}$, the formation of hydroxo-oxalate.

The IR spectrum of the coordination compound (Fig. 1 and Table S1 Electronic Supplementary Material) shows an intense and broad band with the maximum at 3423 cm^{-1} assigned to vibration ν(OH) which confirms the presence of water in the coordination compound [25, 26].

The splitting of the carboxylate vibrations denotes two different coordination modes of the $C_2O_4^{2-}$ ligand: as tetradentate bridge [ν_{asym} (OCO) 1683 cm^{-1}; ν_{sym} (OCO)

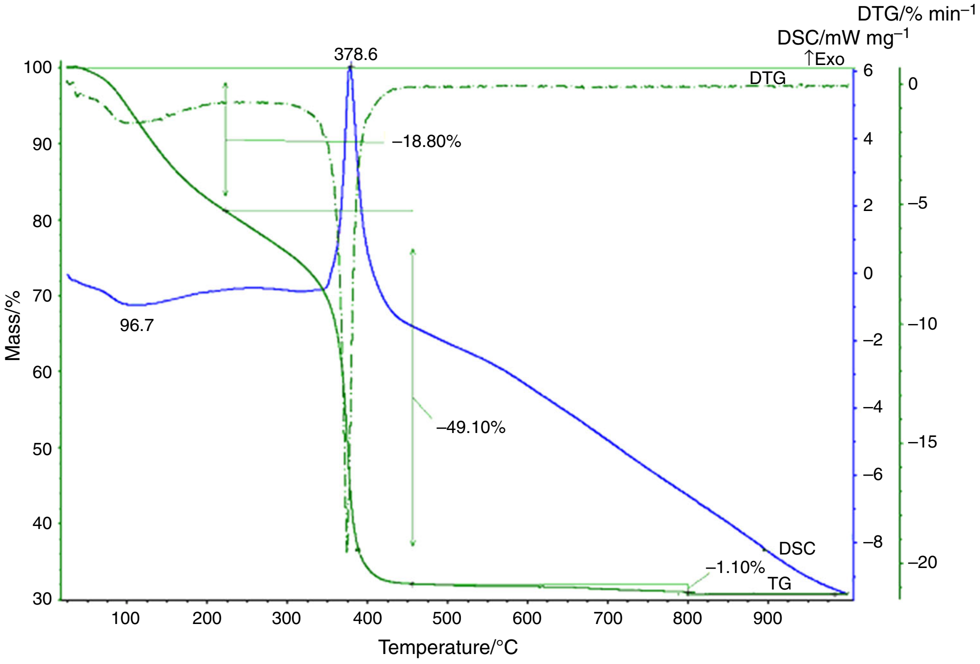

Fig. 2 Thermal curves (TG, DTG and DSC) of $[Al_2Co(C_2O_4)_4(OH_2)_6]$ in air atmosphere (heating rate = 10°/min)

1400–1300 $\mathrm{cm^{-1}}$; δ(OCO) 899 $\mathrm{cm^{-1}}$], and as chelate, bidentate [ν_{asym} (O=C–O) 1707 $\mathrm{cm^{-1}}$; ν_{sym} (O=C–O) 1286 $\mathrm{cm^{-1}}$]. The weak absorption bands in the range 500–400 $\mathrm{cm^{-1}}$ are characteristic for vibrations ν(Al–O) and ν(Co–O). All the results are in good agreement with those from the literature [27].

Nonisothermal behavior of the coordination compound precursor

The thermal decomposition of the investigated coordination compound occurs in the temperature range of 25–1000 °C (Fig. 2) and confirms the formation as end decomposition product a compound with molecular formula of $CoAl_2O_4$ (mass loss calcd./found (%): 69.12/69.00).

The first decomposition stage of the $[Al_2Co(C_2O_4)_4(OH_2)_6]$ compound is attributed to the dehydration process. In the temperature range of 25–222 °C, the six water molecules coordinated were removed (mass loss found/calcd. (%): 18.80/18.85). The second decomposition step (222–456 °C) associated with an exothermic effect (mass loss found/calcd. (%): 49.10/48.99) is assigned to the degradation of the oxalate anion coordinated with the formation of the oxides mixture, Co_3O_4 and Al_2O_3. In the third decomposition step (456–800 °C) the reduction of Co^{3+} to Co^{2+} occurred in the presence of residual carbon, and $CoAl_2O_4$ was obtained (mass loss found/calcd. (%): 1.10/1.28).

Based on the above presented results, this study proposed the following mechanism for the thermal decomposition:

$$3Al_2Co(C_2O_4)_4(OH_2)_6 \xrightarrow{\mathrm{I}} 3Al_2Co(C_2O_4)_4 + 6H_2O$$

$$3Al_2Co(C_2O_4)_4 \xrightarrow{\mathrm{II}} Co_3O_4 + 3Al_2O_3 + 35/2CO_2 + 13/2C$$

$$Co_3O_4 + 1/2C \overset{\mathrm{III}}{\leftrightarrow} 3CoO + 1/2CO_2$$

$$CoO + Al_2O_3 \rightarrow CoAl_2O_4$$

Oxides characterization

Figure 3 presents IR spectra of the products obtained after independent calcinations for 1 h in the temperature range of 500–1000 °C, with a heating rate of 10 °C $\mathrm{min^{-1}}$, in static air atmosphere.

From the IR spectra (Fig. 3) it is observed that for the samples decomposed at 500 and 600 °C appeared the specific bands for Co_3O_4 spinel at 669 and 563 $\mathrm{cm^{-1}}$ [28]. Starting with the samples obtained at 700 °C are evidenced the bands characteristic for $CoAl_2O_4$ spinel (502, 542 and 670 $\mathrm{cm^{-1}}$) [29].

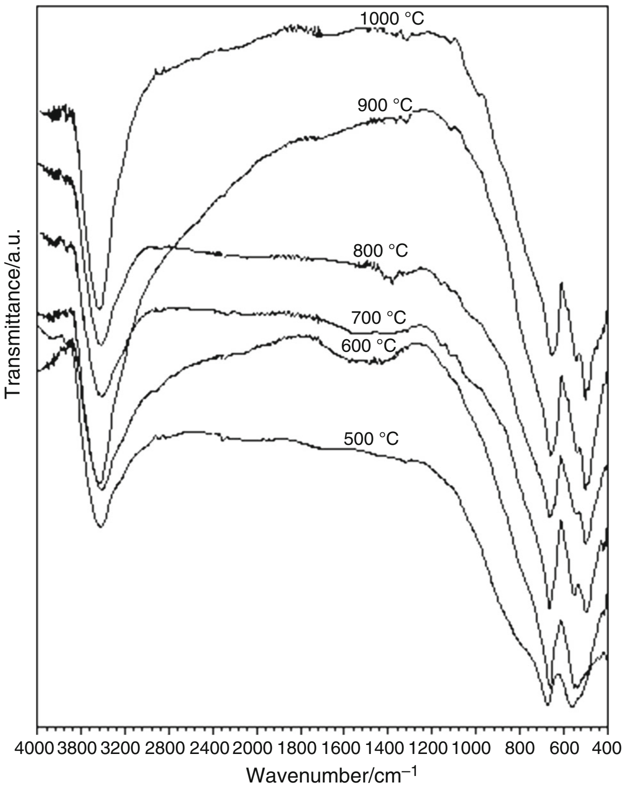

Fig. 3 IR vibrational spectra of products obtained after the calcinations of the coordination compound at various temperatures (500–1000 °C)

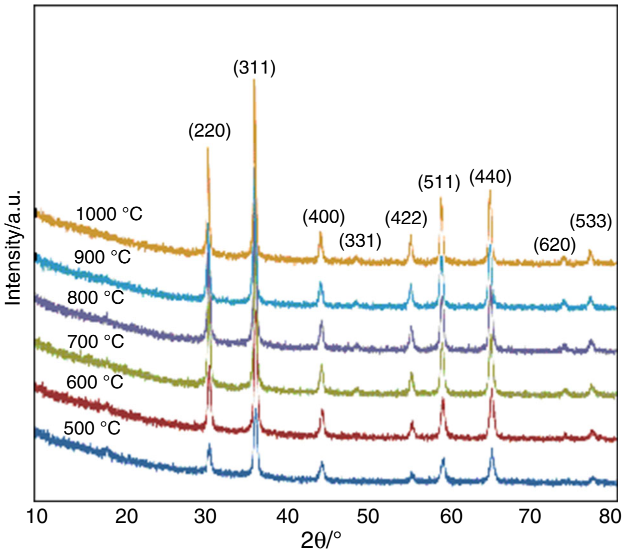

Fig. 4 XRD patterns of products obtained after the calcinations of the coordination compound at various temperatures (500–1000 °C)

The formation of pure $CoAl_2O_4$ after the calcination at 700 °C for 1 h of the coordination compound is also evidenced by XRD patterns presented in Fig. 4. The diffraction lines are in accordance with JCPDS 01-082-2249 file.

As it can be seen, the cobalt aluminate is relatively well crystallized. The formed cobalt aluminate (700 °C) is characterized by a lattice parameter of 8.109 Å, close with the one reported by the literature [30, 31] and an average crystallites size of 16 nm.

TEM image (Fig. 5a) performed on the $CoAl_2O_4$ (700 °C) indicates the formation of small particles, almost homogeneous as shape and size, with a pronounced agglomeration tendency.

The values of the particles sizes obtained by TEM image were in good agreement with the particles size calculated using XRD data, demonstrating the single crystal nature of these particles. The high crystallinity degree is pointed out by the ordered fringes corresponding to the crystalline planes of the spinel structure, as resulted from the HRTEM image presented in Fig. 5b. SAED image revealed the presence of the pure cobalt aluminate and the crystallinity of the particles (Fig. 5c).

Nanosized $CoAl_2O_4$ (700 °C) in sensing application—tetracycline (TC) detection in the aqueous solution

In order to test the suitability for the sensing application, nanosized $CoAl_2O_4$-decorated GC and BDD electrodes were applied for the electrochemical detection of TC in 0.1 M Na_2SO_4 supporting electrolyte. To assess the electrocatalytic effect of $CoAl_2O_4$, the comparative experiments were performed for GC and BDD without any modification of the electrode surface.

The most important aspects regarding the electrocatalytic activity in the detection applications are to shift the detection potential to less positive value and a considerable increase in sensitivity.

Figure 6a, c shows the comparative results for GC and Co–Al–GC electrodes as cyclic voltammetric series

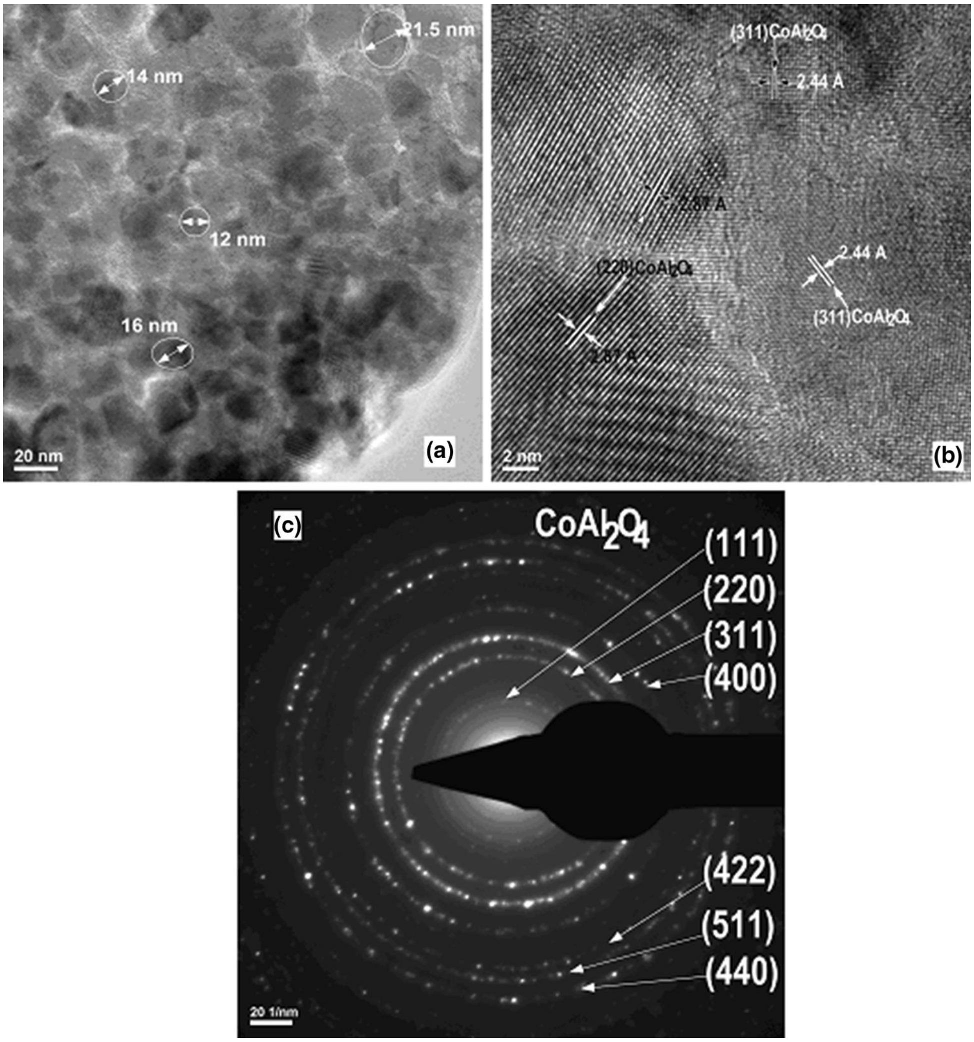

Fig. 5 **a** TEM image, **b** HRTEM image, **c** SAED pattern of the cobalt aluminate obtained after the calcination at 700 °C

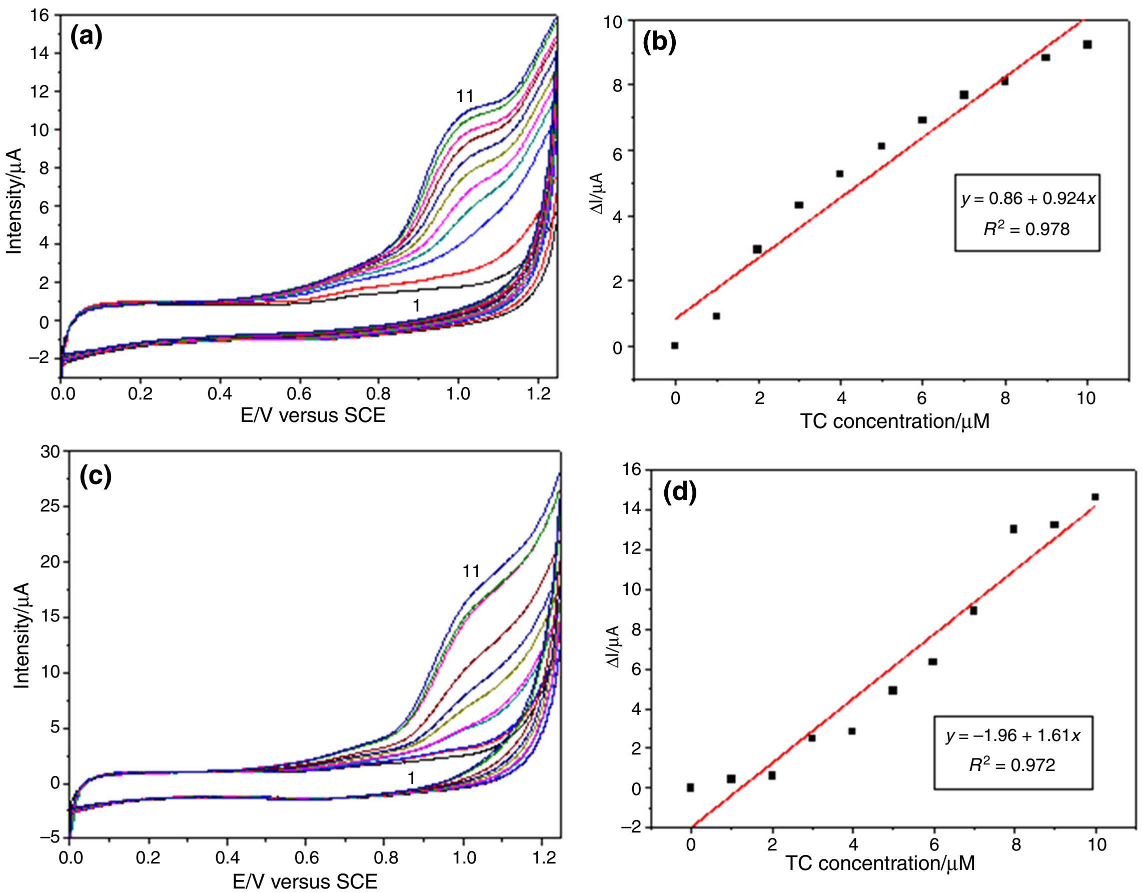

Fig. 6 Cyclic voltammograms recorded in 0.1 M Na_2SO_4 supporting electrolyte (curve 1) and in the presence of 10–100 μM TC (curves 2–11) at a potential scan rate of 0.05 V s^{-1} in a potential range from 0 to 1.25V/SCE using: GC electrode (**a**), and Co–Al–GC (**c**); Calibration plots for the linear dependence of the oxidation peak current recorded at E = +1.05 V/SCE versus TC concentrations for GC electrode (**a**), and Co–Al–GC (**b**)

recorded in the presence of various TC concentrations ranged from 1 to 10 μM.

The oxidation peak corresponding to TC oxidation is noticed at the potential value of +1.05 V/SCE for GC electrode (Fig. 6a), and the oxidation peak currents increased linearly with TC concentration (Fig. 6b). The presence of $CoAl_2O_4$ on the GC surface was not evidenced by CV shape in the presence of 0.1 M Na_2SO_4 supporting electrolyte (curve 1, Fig. 6c), probably due to the small amount of $CoAl_2O_4$. However, the oxidation peak current increased in the presence of $CoAl_2O_4$ and the detection potential is shifted to less positive value in comparison with their absence (1.00 vs. 1.05 V/SCE).

A similar behavior is found for BDD electrode in the presence of TC (Fig. 7).

The presence of $CoAl_2O_4$ on the BDD surface led to more evidenced oxidation peak corresponding to TC oxidation at its same concentration. Also, no oxidation/reduction peaks corresponding to redox process for Co forms were evidence in 0.1 M Na_2SO_4 supporting electrolyte due to low amount of cobalt, which are in according to the results reported for Ni-BDD [22]. However, the oxidation potential and as consequence, the detection potential for TC found in our study is less positive in comparison with one reported (1.00 V vs. 1.4 V/SCE), which could be explained in relation with BDD surface history. Moreover, the CV shape of Co–Al–BDD in the presence of TC is changed in comparison with BDD. The oxidation process of TC started at less positive potential for Co–Al–BDD that represents a characteristic of the electrocatalytic peculiarity.

The comparative results are gathered in Table 1, and it can be easily concluded that for both electrodes the presence of $CoAl_2O_4$ exhibited the electrocatalytic effects toward TC oxidation and detection.

However, the catalytic effect is higher using BDD substrate. The presence of $CoAl_2O_4$ increased the sensitivity for TC detection by about four times for BDD and almost double for GC, which should be explained by the morphology of the substrate and the $CoAl_2O_4$ distribution within the electrode surface.

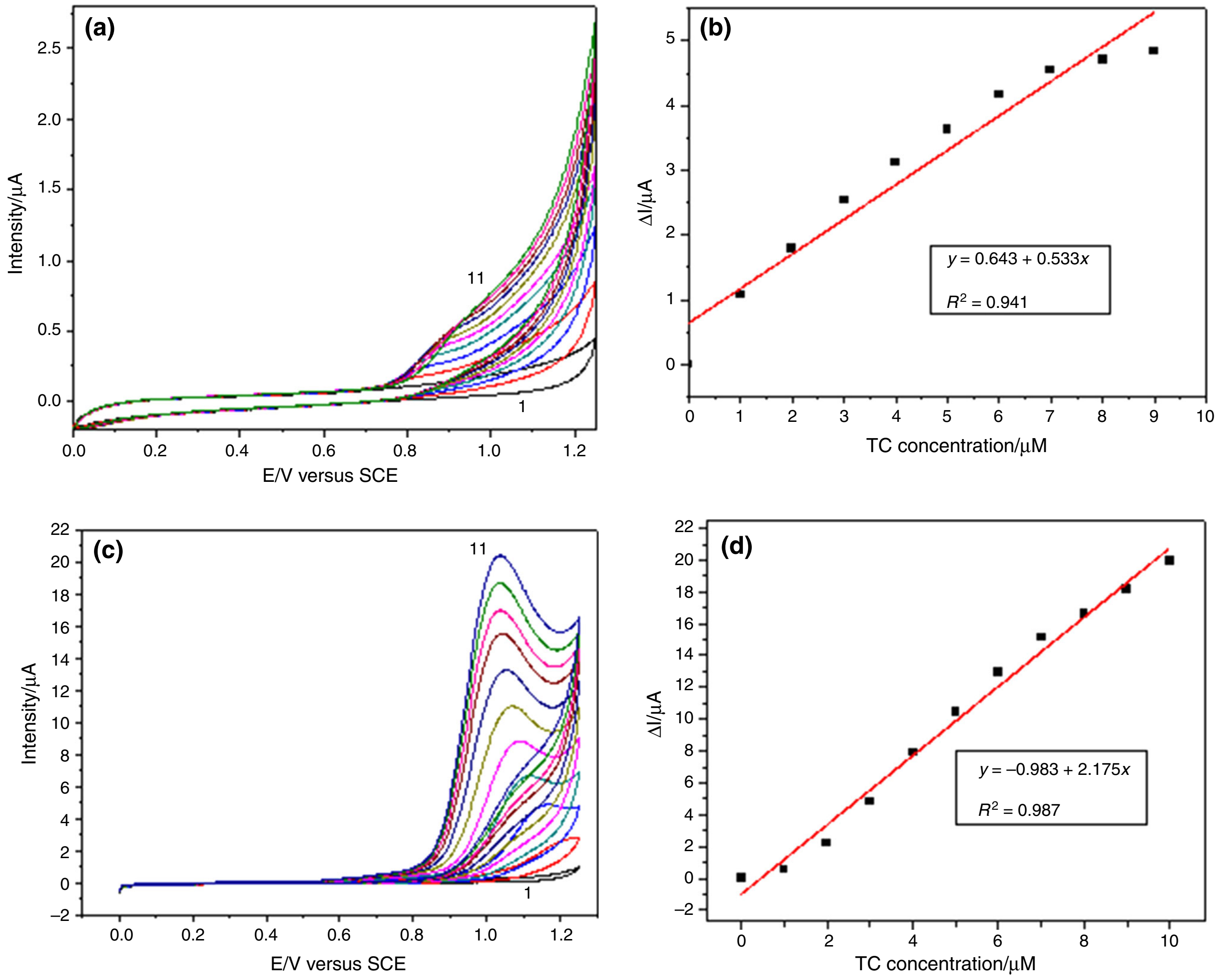

Fig. 7 Cyclic voltammograms recorded in 0.1 M Na_2SO_4 supporting electrolyte (curve 1) and in the presence of 1–10 µM TC (curves 2–11) at a potential scan rate of 0.05 V s^{-1} in a potential range from 0 to 1.25V/SCE using: BDD electrode (**a**), and Co–Al–BDD (**c**); Calibration plots for the linear dependence of the oxidation peak current recorded at E = +0.95 V/SCE versus TC concentrations for BDD electrode (**a**), and Co–Al–BDD (**b**)

Table 1 Detection characteristics determined for TC detection using CV technique

Electrode	Detection potential/V/SCE	Sensitivity/ µA μM^{-1}	Correlation coefficient/R^2
GC	1.05	0.924	0.948
Co–Al–GC	1.00	1.610	0.972
BDD	1.00	0.533	0.943
Co–Al–BDD	1.00	2.175	0.987

Conclusions

Nanosized cobalt aluminate ($CoAl_2O_4$) was obtained through a new method, based on the thermal conversion of oxalate coordination compound at 700 °C. The oxide was identified by IR, XRD and TEM investigations. TEM/HRTEM images indicate the formation of small particles, almost homogeneous as shape and size, with a pronounced agglomeration tendency.

The nanosized $CoAl_2O_4$ (700 °C) exhibited the electrocatalytic activity toward TC oxidation and as consequence, for TC detection for both GC and BDD substrate. The presence of $CoAl_2O_4$ increased the sensitivity for TC detection by about four times for BDD and almost double for GC. This behavior should be explained by better homogeneity of BDD substrate in comparison with GC, which influenced the $CoAl_2O_4$ distribution within the electrode surface.

Acknowledgements "This work was supported by a grant of the Romanian National Authority for Scientific Research and Innovation, CNCS-UEFISCDI, Project Number PN-II-RU-TE-2104-4-1043."

References

1. Eliziario SA, Andrade JM, Lima SJG, Paskocimas CA, Soledade LEB, Hammer P, Longo E, Souza AG, Santos IMG. Black and green pigments based on chromium–cobalt spinels. Mater Chem Phys. 2011;129:619–24.
2. Gawas UB, Verenkar VMS, Mojumdar SC. Nano-crystalline $Mn_{0.3}Ni_{0.3}Zn_{0.4}Fe_2O_4$ obtained by novel fumarato-hydrazinate precursor method: synthesis, characterization and studies of magnetic and electrical properties. J Therm Anal Calorim. 2012;108:865–70.
3. Pawar DK, Pawar SM, Patil PS, Kolekar SS. Synthesis of nanocrystalline nickel-zinc ferrite ($Ni_{0,8}Zn_{0,2}Fe_2O_4$) thin films by chemical bath deposition method. J Alloys Compd. 2011;509: 3587–91.
4. Zawadzki M, Wrzyszcz J. Hydrothermal synthesis of nanoporous zinc aluminate with high surface area. Mater Res Bull. 2000;35:109–14.
5. Li G, Li L, Li Y, Shi J. A highly moisture-resistant Fe-doped mesoporous Co_3O_4 catalyst for efficient low-temperature CO oxidation. New J Chem. 2015;39:1742–8.
6. Queiroz RM, Coelho TL, Queiroz IM, Pires LHO, Santos IMG, Zamian JR, Filho GNR, Costa CEF. Structural and thermal characterization of $Ni_xZn_{12x}Al_2O_4$ synthesized by the polymeric precursor method. J Therm Anal Calorim. 2016;124:1023–8.
7. Deraz NM, Fouda Moustafa MG. Synthesis, structural, morphological properties of cobalt-aluminum nano-composite. Int J Electrochem Sci. 2013;8:2756–67.
8. Souza LKC, Zamian JR, Filho GNR, Soledade LEB, Santos LMG, Souza AG, Scheller T, Angélica RS, Costa CEF. Blue pigments based on $Co \times Zn_{1-x} Al_2O_4$ spinels synthesized by the polymeric precursor method. Dyes Pigm. 2009;81(3):187–92.
9. Rangappa D, Ohara S, Naka T, Kondo A, Ishii M, Adschiri T. Synthesis and organic modification of $CoAl_2O_4$ nanocrystals under supercritical water conditions. J Mater Chem. 2007;17: 4426–9.
10. Carta G, Casarin M, El Habra N, Natali M, Rossetto G, Sada C, Tondello E, Zanella P. MOCVD deposition of $CoAl_2O_4$ films. Electrochim Acta. 2005;50:4592–9.
11. Ji L, Thang S, Zeng HC, Lin J, Tan KL. CO_2 reforming of methane to synthesis gas over sol–gel-made Co/γ-Al_2O_3 catalysts from organometallic precursors. Appl Catal A Gen. 2001;207: 247–55.
12. Ummartyotin S, Sangngern S, Kaewvilai A, Koonsaeng N, Manuspiya H, Laobuthee A. Cobalt aluminate ($CoAl_2O_4$) derived from Co–Al–TEA complex and its dielectric behaviors. J Sustain Energy Environ. 2009;1:31–7.
13. Gama L, Ribeiro MA, Barros BS, Kiminami RHA, Weber IT, Costa ACFM. Synthesis and characterization of the $NiAl_2O_4$, $CoAl_2O_4$ and $ZnAl_2O_4$ spinels by the polymeric precursors method. J Alloys Compd. 2009;483:453–5.
14. Mindru I, Marinescu G, Gingasu D, Patron L, Ghica C, Giurginca M. Blue $CoAl_2O_4$ spinel via complexation method. Mater Chem Phys. 2010;122:491–7.
15. Yu F, Yang J, Ma J, Du J, Zhou Y. Preparation of nanosized $CoAl_2O_4$ powders by sol–gel and sol–gel-hydrothermal methods. J Alloys Compd. 2009;468:443–6.
16. Kang L, He D, Bie L, Jiang P. Nanoporous cobalt oxide nanowires for non-enzymatic electrochemical glucose detection. Sens Actuators B Chem. 2015;220:888–94.
17. Moura SL, Moraes RR, Pereira dos Santos MA, Pividori MI, Lopes JAD, Moreira DL, Zucolotto V, Santos Junior JR. Electrochemical detection in vitro and electron transfer mechanism of testosterone using a modified electrode with a cobalt oxide film. Sensor Actuators B Chem. 2014;202:469–74.
18. Nezamzadeh-Ejhieh A, Pouladsaz P. Voltammetric determination of riboflavin based on electrocatalytic oxidation at zeolite-modified carbon paste electrodes. J Ind Eng Chem. 2014;20:2146–52.
19. Welch CM, Compton RG. The use of nanoparticles in electroanalysis: a review. Anal Bioanal Chem. 2008;391:2469–95.
20. Kushikawa RT, Silva MR, Angelo ACD, Teixeira MFS. Construction of an electrochemical sensing platform based on platinum nanoparticles supported on carbon for tetracycline determination. Sens Actuators B Chem. 2016;228:207–13.
21. Baciu A, Ardelean M, Pop A, Pode R, Manea F. Simultaneous voltammetric/amperometric determination of sulfide and nitrite in water at BDD electrode. Sensors. 2015;15(6):14526–38.
22. Treetepvijit S, Chuanuwatanakul S, Einaga Y, Sato R, Chailapakul O. Electroanalysis of tetracycline using nickel-implanted boron-doped diamond thin film electrode applied to flow injection system. Anal Sci. 2005;2:531–5.
23. Nakamoto K. Infrared and Raman spectra of inorganic and coordination compounds. New York: Wiley; 1986.
24. Dumitru R, Papa F, Balint I, Culita D, Munteanu C, Stanica N, Ianculescu A, Diamandescu L, Carp O. Mesoporous cobalt ferrite: a rival of platinum catalyst in methane combustion reaction. Appl Catal A Gen. 2013;467:178–86.
25. Birzescu M. Ph. D. Thesis, Bucharest Univ., 1998.
26. Fujita J, Nakamoto K, Kobayshi M. Infrared spectra of metallic complexes. II. The absorption bands of coördinated water in Aquo complexes. J Am Chem Soc. 1956;78:3963–5.
27. Bîrzescu M, Niculescu M, Dumitru R, Budrugeac P, Segal E. Copper(II) oxalate obtained through the reaction of 1,2-ethanediol with $Cu(NO_3)_2$ $3H_2O$. J Therm Anal Calorim. 2008;94(1):297–303.
28. Bîrzescu M, Niculescu M, Dumitru R, Carp O, Segal E. Synthesis, structural characterization and thermal analysis of the cobalt(II) oxalate obtained through the reaction of 1,2-ethanediol with $Co(NO_3)_2{\cdot}6H_2O$. J Therm Anal Calorim. 2009;96(3):979–86.
29. Duana X, Panb M, Yua F, Yuan D. Synthesis, structure and optical properties of $CoAl_2O_4$ spinel nanocrystals. J Alloys Compd. 2011;509:1079–83.
30. Wang C, Liu S, Liu L, Bai X. Synthesis of cobalt-aluminate spinels via glycine chelated precursors. Mater Chem Phys. 2006;96:361–70.
31. Mohamed N, Hamed H, Kamal R. The effect of particle size on the kinetics of thermal decomposition of $Co(C_2O_4)$ $2H_2O$ nanopowders under non-isothermal conditions. J Therm Anal Calorim. 2016;123(1):675–86.